Available online at www.sciencedirect.com

ScienceDirect

Proceedings of the Combustion Institute 37 (2019) 5299–5306

Proceedings of the Combustion Institute

www.elsevier.com/locate/proci

Evaluating the impact of uncertainty in flame impulse response model on thermoacoustic instability prediction: A dimensionality reduction approach

Shuai Guo [a,*], Camilo F. Silva [a], Michael Bauerheim [b], Abdulla Ghani [a], Wolfgang Polifke [a]

[a] *Fakultät für Maschinenwesen, Technische Universität München, Boltzmannstr 15, Garching D-85748, Germany*
[b] *Institut Supérieur de l'Aéronautique et de l'Espace, 10 avenue Edouard Belin-BP 54032, Toulouse CEDEX 4 31055, France*

Received 30 November 2017; accepted 7 July 2018
Available online 27 July 2018

Abstract

The flame response to upstream velocity perturbations is properly described by a Finite Impulse Response (FIR) model. When combining an FIR model with acoustic tools to predict thermoacoustic modal growth rates, uncertainties contained in the FIR model coefficients would propagate through the acoustic model, inducing deviations of the modal growth rate from its nominal value. Therefore, an associated uncertainty quantification (UQ) analysis, which focuses on quantifying the impact of FIR model uncertainties on the modal growth rate prediction, is a necessity to obtain a more reliable thermoacoustic instability prediction. To address this UQ problem, our present work proposes an analytical strategy featuring (1) compactly summarizing the causal relationship between variations of FIR model coefficients and variations of modal growth rates; (2) Effectively shrinking the dimension of the UQ problem; (3) Requiring only negligible computational cost; (4) Involving no complex mathematical treatments. Our case studies yielded 5000 times faster yet highly accurate UQ analyses compared with reference Monte Carlo simulations, even though a significant level of FIR model uncertainty is present. The analytical approach brings additional benefits including (1) visualization of the process from the variations of FIR model coefficients to the variations of modal growth rate; (2) Easily-obtainable sensitivity measurement for each FIR model coefficient, which can help identify key mechanisms controlling the thermoacoustic instability; (3) New possibility for robust combustor design, i.e., to minimize the impact of FIR model uncertainty on the thermoacoustic instability prediction.

Keywords: Uncertainty quantification; Flame impulse response model; Thermoacoustic instability; Dimensionality reduction

1. Introduction

Combining acoustic tools (e.g., Helmholtz solvers [1] or network models [2]) with a flame

* Corresponding author.
E-mail address: guo@tfd.mw.tum.de (S. Guo).

https://doi.org/10.1016/j.proci.2018.07.020

response model is a popular approach to predict thermoacoustic instability. In this framework, the flame response model, which may be derived from experiment or numerical simulation, constitutes a source of uncertainty, which may have significant impact on the reliability of modal growth rate calculation, as is evidenced by the work of Nair et al. [3], Ndiaye et al. [4], Bauerheim et al. [5], Magri et al. [6] as well as Silva et al. [7]. In these studies, 2-coefficient $n-\tau$ models [8] were investigated, and the gain n and the time delay τ of the flame response were considered as uncertain input parameters.

Compared with a frequency-independent $n-\tau$ model, the finite impulse response (FIR) model represents a more sophisticated and realistic flame model, which describes flame dynamics in the time domain and facilitates direct physical interpretation of flow-flame interaction mechanisms [9]. In fact, the $n-\tau$ model can be viewed as a special case of an FIR model with only one non-zero coefficient. FIR models can be deduced from experimentally measured flame frequency response data [10] or determined through a combined CFD/System Identification procedure [11]. To further pave the way for using this advanced flame response model, it is essential to quantify the impact of uncertainties in the FIR model and obtain the associated error in predicting thermoacoustic instability. Uncertainty quantification (UQ) analysis, which focuses on propagating uncertainties from inputs to outputs, is required for that purpose.

Monte Carlo simulation [12] is a classic method for conducting UQ analysis. However, due to its slow convergence, a large number of samples (generally in the order of thousands) have to be drawn from the distribution of inputs and an equally large number of model evaluations are required to construct a converged probability density function (PDF) of the output. Therefore, previous studies investigating the impact of uncertain flame model have employed various sophisticated surrogate techniques [4–7,12], so that a smaller number of input samples and corresponding model evaluations is sufficient for UQ analysis.

In this work we propose a dimensionality reduction strategy based on analytical analysis to address our current UQ problem, i.e., evaluate the impact of FIR model uncertainties on the thermoacoustic modal growth rate calculation, so that we can (1) perform UQ analysis analytically to improve the efficiency, while avoiding sophisticated mathematical treatments as much as possible; (2) obtain further physical insights regarding the causal relationship between FIR model coefficient variations and modal growth rate variations. This paper starts with a statement of our current UQ problem, followed by introducing the way we visualize the results. Then we derive the dimensionality reduction strategy and demonstrate its effectiveness through case studies. We close the paper by pointing out further applications of the proposed UQ strategy.

2. UQ problem setting

In the present study, we investigate the uncertainty regarding the growth rate of a marginally stable thermoacoustic mode in a combustor computed with an acoustic network solver. An FIR model is introduced to describe the flame response, which links velocity fluctuations u'_u upstream of the flame to the global heat release rate fluctuations $\dot{Q}'$ in the following manner:

$$\frac{\dot{Q}'_n}{\bar{\dot{Q}}} = \frac{1}{\bar{u}_u}\sum_{k=0}^{L-1} h_k u'_{u,n-k} \tag{1}$$

where h_k's are the FIR model coefficients, which are considered uncertain. L is the model order (i.e. number of coefficients) and n is the time step. The overbar and the prime indicate average and fluctuating values, respectively.

The uncertainty of the FIR model coefficients stems from their estimation process, either through experimental measurements, which inevitably contains noise, or through a combined approach of CFD/System-identification [11], where (1) CFD simulation can be uncertain, e.g., boundary conditions, combustion model parameters, etc. and (2) identification process will be uncertain, e.g., due to its stochastic nature, low signal-to-noise ratio, finite length of CFD time series [13], etc. As a result, the estimation results for h_k's containing not only nominal values, but also an associated covariance matrix which describes the uncertainty information of h_k's. In the present work, we assume that the FIR model uncertainty is known.

Conventional thermoacoustic instability prediction only employs the nominal values h_k^0's (nominal quantities are denoted by superscript "0", the same hereinafter) and calculates the corresponding eigenvalues of the thermoacoustic system $(\boldsymbol{i}\omega^0+\sigma^0)\in\mathbb{C}$, *i.e.,* modal frequency $\omega^0\in\mathbb{R}$ and growth rate $\sigma^0\in\mathbb{R}$. This analysis is also referred to as deterministic analysis. However, conducting only deterministic analysis can be dangerous for marginally stable thermoacoustic modes [4–7], since they can become unstable when h_k's deviate from their nominal values.

In contrast to the deterministic analysis, UQ analysis takes into account variations of FIR model coefficients and propagates their uncertainties to the output, in particular, the modal growth rate σ. Therefore, the output is not just a single value σ^0, but a PDF, which describes the output in a statistical manner.

By means of the Monte Carlo method, a large number of samples of FIR model coefficients have to be drawn from the distribution of coefficients, and for each sample the corresponding modal

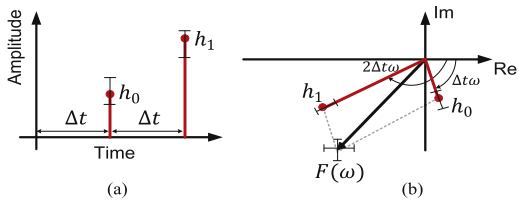

Fig. 1. The sketch of (a) a simplified FIR model and (b) the phasor plot of FRF.

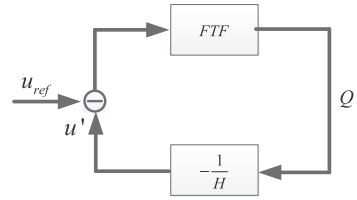

Fig. 2. The thermoacoustic closed-loop network.

growth rate has to be calculated. Clearly, direct Monte Carlo requires a large number of model evaluations, thus making it a possibly very expensive method.

3. Results visualization - phasor plot of FRF

Before addressing our current UQ problem, firstly, we need to introduce the phasor plot of the flame frequency response function (FRF), which lays the foundation for illustrating the results in the reminder of this paper.

The FRF describes the flame dynamics in frequency domain and is obtained from the general flame transfer function (FTF) in complex domain by setting the growth rate σ in FTF to zero. FRF can be obtained from the FIR model as in Eq. (2) [11], where the h_k's are the corresponding FIR model coefficients, $\omega \in \mathbb{R}$ denotes the frequency and Δt represents the sampling interval between successive FIR model coefficients.

$$\mathrm{F}(\omega) = \sum_{k=0}^{L-1} h_k e^{-\boldsymbol{i}(k+1)\Delta t\omega}, \quad \omega \in \mathbb{R} \tag{2}$$

For illustration, we consider a simplified FIR model in Fig. 1a, with only two coefficients (h_0 and h_1) as well as their uncertainty bounds. In this case, when F is evaluated at a fixed nominal frequency ω^0, Eq. (2) is written as:

$$\mathrm{F}(\omega^0) = h_0 e^{-\boldsymbol{i}\Delta t\omega^0} + h_1 e^{-\boldsymbol{i}(2\Delta t)\omega^0} \tag{3}$$

Therefore we can draw $\mathrm{F}(\omega^0)$ in Eq. (3) in Fig. 1b, which we refer to as the phasor plot of FRF. Since the values of h_k's are uncertain, any variations of the coefficient h_k will cause change of length of the respective phasor. Consequently, the length and direction of the $\mathrm{F}(\omega^0)$ phasor will change too.

We use the term *sample* to refer to one particular combination of h_k's, i.e., sample $\boldsymbol{h} = \{h_0, h_1, \ldots, h_{L-1}\}$. We are particularly interested in (1) sets of samples, that produce the same modal growth rate, and (2) the head locations of their corresponding F phasor evaluated at the fixed nominal frequency ω^0. In other words, we focus on the distribution pattern of the iso-growth lines in the phasor plot of FRF.

4. Analytical UQ procedure derivation

In this section, we demonstrate the analytical derivation and prove that to first-order, the isolines of growth rate of thermoacoustic instability are parallel straight lines in the phasor plot of FRF. Then, we discuss why this finding is crucial for addressing the current UQ problem setting in an analytical way. Finally, we summarize the analytical procedure.

4.1. Iso-growthlines in the phasor plot of FRF

The thermoacoustic system is a closed-loop network. As shown in Fig. 2, we choose the velocity at a reference location just upstream of the flame as the input and global heat release fluctuation as the output. The block *FTF* describes the link between velocity fluctuation and global heat release fluctuation, while the block $-1/H$ describes the acoustic response of the combustor to the global heat release fluctuation. Consequently, we can derive the characteristic equation of the system [14]:

$$FTF(\omega - \boldsymbol{i}\sigma) = H(\omega - \boldsymbol{i}\sigma) \quad \omega, \sigma \in \mathbb{R} \tag{4}$$

Since we are using an FIR model, Eq. (4) can be written as:

$$\sum_{k=0}^{L-1} h_k e^{-\boldsymbol{i}(k+1)\Delta t(\omega - \boldsymbol{i}\sigma)} = H(\omega - \boldsymbol{i}\sigma) \tag{5}$$

We argue that terms $e^{-(k+1)\Delta t\sigma}, k = 0...(L-1)$ can be approximated as 1 since: (1) $L\Delta t$, the flame response time to the velocity perturbation, is normally at the order of milliseconds; (2) we consider marginally stable thermoacoustic modes, which means the growth rates σ is close to zero. Therefore Eq. (5) may be approximated as:

$$\sum_{k=0}^{L-1} h_k e^{-\boldsymbol{i}(k+1)\Delta t\omega} = H(\omega - \boldsymbol{i}\sigma) \tag{6}$$

For any perturbed sample $\boldsymbol{h^*} = \boldsymbol{h^0} + \Delta\boldsymbol{h}$, we have the corresponding modal frequency $\omega^* = \omega^0 + \Delta\omega$ and growth rate $\sigma^* = \sigma^0 + \Delta\sigma$. We substitute $\boldsymbol{h^*}$, ω^* and σ^* into Eq. (6), perform first-order Taylor expansion around the nominal on both sides of the equation, and then combine like

terms:

$$\underbrace{\left(\boldsymbol{i}\sum_{k=0}^{L-1}\Delta t(k+1)h_k^0 e^{-\boldsymbol{i}(k+1)\Delta t\omega^0}+\left.\frac{\partial H}{\partial\omega}\right|^0\right)\Delta\omega}_{G^0=G_r^0+\boldsymbol{i}G_i^0}+\left.\frac{\partial H}{\partial\sigma}\right|^0\Delta\sigma=\sum_{k=0}^{L-1}\Delta h_k e^{-\boldsymbol{i}(k+1)\Delta t\omega^0} \tag{7}$$

where "$|^0$" indicates evaluation using corresponding nominal values.

Now we consider two specific perturbed samples $\boldsymbol{h}'$ and $\boldsymbol{h}''$, with their modal frequencies and growth rates being (ω', σ') and (ω'', σ''). We want to determine under which condition the modal growth rate of these two samples are the same. To achieve that, we expand their characteristic equations as in Eq. (7) and subtract the two expanded characteristic equations from each other:

$$\delta\omega G^0+\delta\sigma\left.\frac{\partial H}{\partial\sigma}\right|^0=\sum_{k=0}^{L-1}\delta h_k e^{-\boldsymbol{i}(k+1)\Delta t\omega^0} \tag{8}$$

where $\delta h_k=h_k'-h_k''$, $\delta\omega=\omega'-\omega''$ and $\delta\sigma=\sigma'-\sigma''$. The r.h.s term in Eq. (8) can be written as:

$$\sum_{k=0}^{L-1}\delta h_k e^{-\boldsymbol{i}(k+1)\Delta t\omega^0}=\delta F_r+\boldsymbol{i}\delta F_i \tag{9}$$

where δF_r and δF_i represent the F(ω^0) phasor displacement along the real and imaginary axes of the phasor plot of the FRF, when the coefficients of FIR change from $\boldsymbol{h}'$ to $\boldsymbol{h}''$. Also, $H(\omega-\boldsymbol{i}\sigma)$ can be explicitly written as $H(\omega-\boldsymbol{i}\sigma)=H_r(\omega,\sigma)+\boldsymbol{i}H_i(\omega,\sigma)$. Therefore, we can re-express Eq. (8) in its real part and imaginary part as a system of linear equations, with $\delta\omega$ and $\delta\sigma$ being the unknowns:

$$\begin{pmatrix}G_r^0 & \left.\frac{\partial H_r}{\partial\sigma}\right|^0\\ G_i^0 & \left.\frac{\partial H_i}{\partial\sigma}\right|^0\end{pmatrix}\begin{pmatrix}\delta\omega\\ \delta\sigma\end{pmatrix}=\begin{pmatrix}\delta F_r\\ \delta F_i\end{pmatrix} \tag{10}$$

where:

$$G_r^0=\left.\frac{\partial H_r}{\partial\omega}\right|^0+\sum_{k=0}^{L-1}h_k^0(k+1)\Delta t\sin[(k+1)\Delta t\omega^0] \tag{11}$$

$$G_i^0=\left.\frac{\partial H_i}{\partial\omega}\right|^0+\sum_{k=0}^{L-1}h_k^0(k+1)\Delta t\cos[(k+1)\Delta t\omega^0] \tag{12}$$

To obtain the iso-growth lines, the solution for $\delta\sigma$ in Eq. (10) should be zero, which requires:

$$G_i^0\delta F_r-G_r^0\delta F_i=0 \tag{13}$$

Eq. (13) represents a line equation in the phasor plot of FRF for given G_r^0 and G_i^0, with the line direction $\boldsymbol{l}=(G_r^0,G_i^0)$ and corresponding normal direction $\boldsymbol{n}=(G_i^0,-G_r^0)$, as sketched in Fig. 3. For

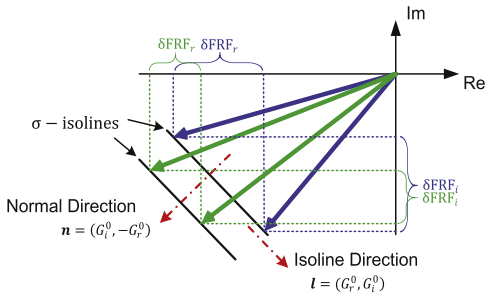

Fig. 3. Two pairs (blue and green) of perturbed samples are plotted in the phasor plot of FRF. Within each pair, two samples yield same modal growth rate and the head locations of their corresponding F phasors are along a straight line; Across pairs, these straight lines are in parallel. (For interpretation of the references to color in this figure legend, the reader is referred to the web version of this article.)

any two perturbed samples of $\boldsymbol{h}$, as long as they fulfill Eq. (13), they will yield to first order the same modal growth rate. Therefore, we can conclude that the iso-growth lines in the phasor plot of FRF are approximately a set of parallel straight lines approximately. Here we emphasis that (1) G_r^0 and G_i^0 are determined by the FIR model, plus the transfer function of the acoustic model (H) of the thermoacoustic system, as well as the specific thermoacoustic mode (ω^0 and σ^0). Therefore, when (a) different FIR model is employed or (b) geometry or boundary conditions of the combustor are altered or (c) different thermoacoustic modes are investigated, these directions are expected to be different; (2) it can be shown that the mathematical derivation above is also valid when a simple $n-\tau$ flame model is adopted, where both n and τ exhibit uncertainties. The same conclusion is reached eventually, *i.e.,* iso-growth lines in the phasor plot of the FRF are to first order a set of parallel straight lines to first order.

4.2. Analytical results discussion

Now we are ready to exploit the analytical results for conducting UQ analysis. As shown in Fig. 4 (same simplified FIR model as in Fig. 1): (1) When perturbing individual FIR model coefficient (Δh_0 and Δh_1), the head location of the F(ω^0) phasor in general moves to a different level of modal growth rate. This helps to visualize the causal relationship between the FIR model coefficient variations and the modal growth rate variation; (2) Each coefficient's variation can modify the modal growth rate individually. Nevertheless, what ultimately determines the modal growth rate change is the sum of the projection of each phasor $(h_k-h_k^0)e^{-\boldsymbol{i}(k+1)\Delta t\omega^0}$ on the normal direction of the contours of modal growth rate. We use

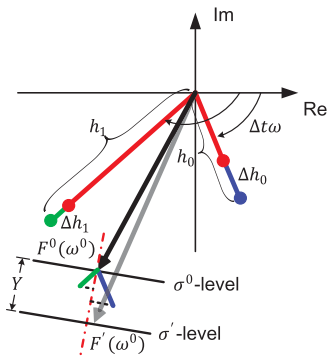

Fig. 4. Visual demonstration of the causal relationship between the variations of FIR model coefficients and the variations of modal growth rate.

Y to denote this projection sum, which can formally be written in Eq. (14). Here $\boldsymbol{n}$ is the normal direction of the iso-growth lines (as indicated in Fig. 3).

$$Y = \sum_{k=0}^{L-1} (h_k - h_k^0) e^{-\boldsymbol{i}(k+1)\Delta t\omega^0} \cdot \frac{\boldsymbol{n}}{|\boldsymbol{n}|} \tag{14}$$

Therefore, we can relate the FIR model coefficient variations to the modal growth rate variation in the following manner:

$$\sigma = f(Y) \tag{15}$$

where the surrogate function $f()$ represents a one-to-one mapping from a specific value of Y, which is the distance (can be negative) along the normal direction of the iso-growth lines starting from the head location of the nominal F phasor evaluated at nominal frequency ω^0, to a specific value of the modal growth rate variation.

At this point we can see that the modal growth rate σ of any sample $\boldsymbol{h}$ is expressed as an univariate function of Y, which depends on nominal coefficients $\boldsymbol{h^0}$ and the nominal eigen-frequency $\boldsymbol{\omega^0}$, but is essentially a linear combination of h_k's (Eq. (14)). For the current UQ problem, the L input variables (the number of h_k's is L) can be condensed into a single variable Y, thus, a potentially very significant dimensionality reduction is achieved. Interestingly, a one-dimensional structure similar to Y was also identified through Active Subspace approach [12], which is a mathematically much more demanding method.

4.3. An analytical UQ strategy

Here we outline the steps for the analytical UQ strategy, assuming that the nominal values and distributions for FIR model coefficients are known, and acoustic network model has already been set up.

Step 1: Perform deterministic thermoacoustic stability analysis to obtain the nominal frequency ω^0 and modal growth rate σ^0 of the interested thermoacoustic mode.

Step 2: Calculate the normal direction of the iso-growth lines $\boldsymbol{n}$.

Step 3: Construct function $f()$ in Eq. (15) in the following manner:

Step 3.1: Draw several samples (5–10) of FIR model coefficients from their distribution, obtain their Y values. Here we suggest the following way to determine those FIR coefficient samples: (a) draw a large number of FIR coefficient samples (e.g., 10^4 samples, store as the data bank), calculate their corresponding Y values; (b) Estimate Y's cumulative distribution function, employ space-filling sampling method (e.g., Latin Hypercube, Halton or Sobol sequences) to draw several (5–10) "ideal" samples for Y which satisfy the experimental design criteria; (c) Find those FIR coefficient samples in the data bank whose Y values are closest to the "ideal" Y sample;

Step 3.2: Calculate the modal growth rate of each sample (in *Step 3.1*) using thermoacoustic system model;

Step 3.3: Plot the modal growth rate values against corresponding Y values and fit a function f (i.e., polynomial, Kriging, Radial basis function, etc.);

Step 4: Perform standard Monte Carlo simulation, i.e., draw a large amount of samples of FIR model coefficients, for each sample, first calculate its Y value through Eq. (14), then calculate the corresponding modal growth rate through Eq. (15). Based on the obtained data bank of the modal growth rate values, a PDF can be constructed and relevant statistical indices can be extracted.

To summarize, the analytical approach manages to uncover a one-dimensional approximation (summarized as Y) of the original system, and take very few potentially expensive thermoacoustic system calculations (1 in *Step 1* and 5–10 in *Step 3.2*) to build a surrogate model only upon Y. Subsequent Monte Carlo simulations can be applied directly on this one-dimensional surrogate model, thus, achieving a significantly accelerated UQ analysis.

5. Application of analytical UQ strategy to combustion test rig

This section aims to demonstrate the accuracy and effectiveness of the UQ strategy proposed in Section 4.3. We investigate the uncertainty regarding the modal growth rate of the BRS burner [15] using an acoustic network solver combined with a 16-coefficient FIR model, assuming that the FIR model coefficients are the only source of uncertainty. The only reason for adopting a simple yet practical acoustic network model here is that brutal force Monte Carlo is entirely feasible so that we can verify our approach.

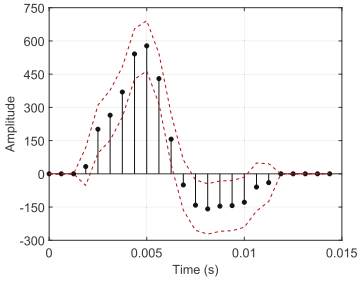

Fig. 5. Finite impulse response model. Each discrete stem represents one coefficient h_k, upper and lower red dot line constitute the 95% confidence interval. (For interpretation of the references to color in this figure legend, the reader is referred to the web version of this article.)

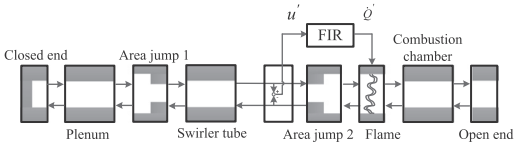

Fig. 6. Sketch of the acoustic network model. Flow from left to right.

5.1. Thermoacoustic model

Figure 5 displays the 16-coefficient FIR model adopted in the current study, which includes both the nominal value and 95% confidence interval for each coefficient. The FIR model is identified using the procedure described in Keesman [16], based on the LES data of [17], where velocity perturbations at the burner mouth u' and global heat release rate fluctuations $\dot{Q}'$ are recorded and considered as input and output, for the identification procedure, respectively. In the current UQ analysis, each FIR model coefficients are treated as a random variable, and they follow multivariate normal distribution. The covariance matrix of the FIR model coefficients is also obtained from the identification process.

The acoustic network model of the BRS burner is sketched in Fig. 6. The geometrical and thermodynamic parameters are given in [12]: two pairs of chamber length values ($l_A = 0.51$ m and $l_B = 0.6$ m) and reflection coefficient values for the combustor exit ($R_A = -0.98$ and $R_B = -0.63$) are selected and marked as case A and case B, respectively. The transfer matrix for each acoustic element and their assembly are given in [2].

Here we focus on evaluating the impact of uncertain FIR model on the dominant mode (with largest modal growth rate) of each case, which are shown in Fig. 7. These modes are calculated with standard deterministic analysis. When FIR model uncertainty is considered, these dominant modes may become unstable, since they are relatively close

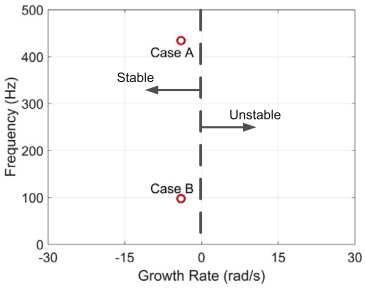

Fig. 7. Thermoacoustic modes calculated by deterministic analysis. For case A, the nominal modal frequency is 434.2 Hz and growth rate is −4 rad/s. For case B, the corresponding values are 97.5 Hz and −4 rad/s.

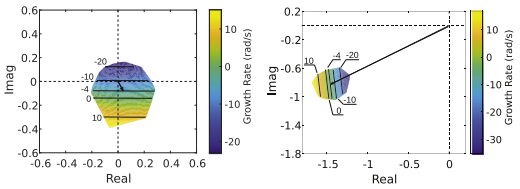

(a) Case A (b) Case B

Fig. 8. Modal growth rate contours in generalized phasor plot of FRF. Black lines are the contour levels predicted by the analytical approach. For each case, Line with black arrow is the $F(\omega^0)$ phasor evaluated by using nominal values of h_k's, which corresponds to a growth rate value of −4 rad/s.

to the stability limit, thus highlighting the necessity of UQ analysis.

5.2. UQ analysis

First we assess if the parallel straight lines (Eq. (13)) are good approximations of the iso-growth lines in the phasor plot of FRF. Here we treat the acoustic network calculation as the full accuracy/reference solution, and its prediction of the iso-growth lines for both cases are plotted in Fig. 8. We drew 5000 samples of $\boldsymbol{h}$ for each case and for each sample we calculated the corresponding modal growth rate by acoustic network model as well as the coordinates of $F(\omega^0)$ in the phasor plot, based on which we can construct the iso-growth lines. We emphasize that such large number of samples is only necessary for this verification study, but not for the application of our proposed UQ approach. We can see from Fig. 8 that parallel straight lines, as indicated by analytical results, indeed capture the essence of the distribution of the iso-growth lines.

Following Section 4.3, we employ the analytical strategy to conduct UQ analysis. One critical step is ***Step 3***, i.e., constructing a surrogate function $f()$ to map Y value to modal growth rate value. For that purpose, we fit a quadratic function based on

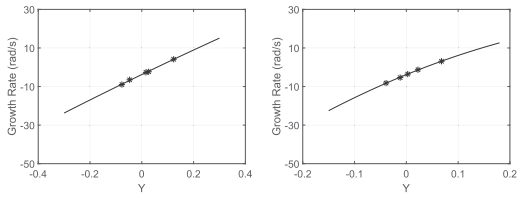

(a) Case A (b) Case B

Fig. 9. For each case, a quadratic function is fitted to link Y to modal growth rate.

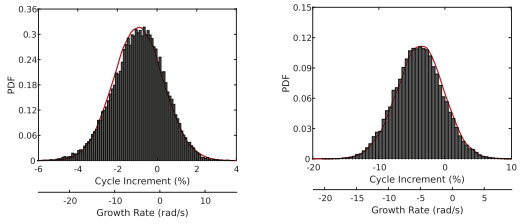

(a) Case A (b) Case B

Fig. 10. PDF comparison between analytical results (red curves) and benchmark Monte Carlo results (bars). (For interpretation of the references to color in this figure legend, the reader is referred to the web version of this article.)

5 samples of FIR model coefficients for each case, which is shown in Fig. 9.

Figure 10 compares the PDF of the modal growth rate predicted by the analytical approach and benchmark Monte Carlo, which is based on 30,000 full-accuracy acoustic network evaluations. Corresponding cycle increments [18] of the thermoacoustic modes are also given to show the relative amplitude change per cycle.

Here it can be seen that our proposed analytical UQ strategy, though it is based on a first-order approximation, is very efficient and robust since: (1) our approach requires very few expensive thermoacoustic system evaluations; (2) in the cases studies, the uncertainty level of the adopted FIR model can already be considered as large (the maximum ratio of coefficient standard deviation to coefficient mean can be as large as 130%), yet our approach still managed to reproduce the benchmark Monte Carlo results; (3) for practical usage, the uncertainty level of the FIR model should not be larger than what we presented here, thus posing less challenge for the proposed UQ approach.

6. Conclusion

In the framework of evaluating the impact of FIR model uncertainties on the thermoacoustic instability prediction, our current work managed to uncover a one-dimensional approximation of the original thermoacoustic system, which compactly

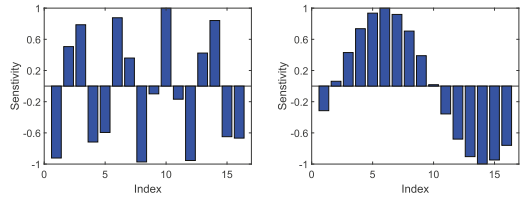

(a) Case A (b) Case B

Fig. 11. Sensitivity measurements for each FIR model coefficients.

summarized the causal relationship between the variations of FIR model coefficients and the variations of thermoacoustic modal growth rate, and proposed a dimensionality strategy to address this UQ problem analytically. Only a handful of thermoacoustic system evaluations are required to accurately build a PDF of the growth rate of the investigated thermoacoustic mode, thus achieving dramatic efficiency improvement, while avoiding any complex mathematical treatments normally employed in other sophisticated surrogate modelling techniques. It should be noted that the convenience of the analytical procedure exposed in this work for affordable UQ studies becomes evident when considering more complex acoustic models, like the ones characterized by the Helmholtz Equation or the Linearized Navier–Stokes Equation, where a single computation is considerably more expensive than the one of a simple acoustic network model. In such models, the acoustic transfer function $H(\omega - i\sigma)$ (see Fig. 2) is directly linked to local values of the system matrix (the acoustic operator) and, therefore, readily obtainable. In addition, the analytical results can be further exploited in the following two areas:

- Sensitivity analysis: The analytical approach provides the sensitivity measurement of modal growth rate against each FIR model coefficient S_k, which can be seen as the ability of each FIR model coefficient to modify the modal growth rate, and can be formally written as:

$$S_k = e^{-j(k+1)\Delta t\omega^0}\frac{\boldsymbol{n}}{|\boldsymbol{n}|}, \quad k = 0, \ldots L-1 \qquad (16)$$

  For the purpose of illustration, the sensitivity measurement of each FIR model coefficient for both cases (case A and case B in Section 5.1) are plotted in Fig. 11. As described in [9], FIR model coefficients contain insightful information regarding the flow-flame interaction. Now equipped with easily-obtainable sensitivity measurements, it may help to identify the key mechanisms controlling the modal growth rate and enhance our understanding of the relevant physical phenomenon.
- Robust design: In some occasions, we are interested in optimizing combustor

geometries and boundary conditions to minimize the impact of uncertain FIR model on the modal growth rate prediction. The underlying difficulty is the determination of the modal growth rate variation. Now with the capability of performing UQ analysis analytically, this index can be easily obtained with only a few thermoacoustic system calculations within each optimization algorithm loop, which could lead to a significantly accelerated optimization process.

Acknowledgments

S. Guo is grateful for the financial support from doctoral scholarship of Chinese Scholarship Council (No. 201606830045). W. Polife and C. Silva are grateful to the 2014 Center for Turbulence Research Summer Program (Standford University), where discussions with Franck Nicoud instigated the ideas developed in this study.

References

[1] F. Nicoud, L. Benoit, C. Sensiau, T. Poinsot, *AIAA J.* 45 (2) (2007) 426–441, doi:10.2514/1.24933.
[2] C.F. Silva, T. Emmert, S. Jaensch, W. Polifke, *Combust. Flame* 162 (9) (2015) 3370–3378, doi:10.1016/j.combustflame.2015.06.003.
[3] V. Nair, S. Sarkar, R.I. Sujith, *Probab. Eng. Mech.* 34 (2013) 177–188, doi:10.1016/j.probengmech.2013.09.005.
[4] A. Ndiaye, M. Bauerheim, F. Nicoud, in: Proceedings of the Turbine Technical Conference and Exposition, ASME Turbo Expo, in: GT2015-44133, ASME, Montreal, Quebec, Canada, 2015.
[5] M. Bauerheim, A. Ndiaye, P. Constantine, S. Moreau, F. Nicoud, *J. Fluid Mech.* 789 (2016) 534–566, doi:10.1017/jfm.2015.730.
[6] L. Magri, M. Bauerheim, F. Nicoud, M.P. Juniper, *J. Comput. Phys.* 325 (2016) 411–421, doi:10.1016/j.jcp.2016.08.043.
[7] C. Silva, L. Magri, T. Runte, W. Polifke, *J. Eng. Gas Turb. Power* 139 (1) (2017) 011901, doi:10.1115/1.4034203.
[8] L. Crocco, *J. Am. Rocket Soc.* 21 (6) (1951) 163–178.
[9] R.S. Blumenthal, P. Subramanian, R. Sujith, W. Polifke, *Combust. Flame* 160 (7) (2013) 1215–1224, doi:10.1016/j.combustflame.2013.02.005.
[10] P. Subramanian, R.S. Blumenthal, R. Sujith, W. Polifke, *Combust. Theory Model.* 19 (2) (2015) 223–237, doi:10.1080/13647830.2014.1001438.
[11] W. Polifke, *Ann. Nuclear Energy* 67C (2014) 109–128, doi:10.1016/j.anucene.2013.10.037.
[12] S. Guo, C.F. Silva, A. Ghani, W. Polifke, in: Proceedings of the Turbomachinery Technical Conference & Exposition, ASME Turbo Expo, in: GT2018-75644, ASME, Lillestrom, Norway, 2018.
[13] C. Sovardi, S. Jaensch, W. Polifke, *J. Sound Vibr.* 377 (2016) 90–105, doi:10.1016/j.jsv.2016.05.025.
[14] B. Schuermans, H. Luebcke, D. Bajusz, P. Flohr, in: Proceedings of the ASME Turbo Expo, in: GT2005-68393, ASME, Reno, Nevada, USA, 2005, doi:10.1115/GT2005-68393.
[15] T. Komarek, W. Polifke, *J. Eng. Gas Turb. Power* 132 (6) (2010) 061503, doi:10.1115/1.4000127.
[16] K.J. Keesman, in: System Identification, in: Advanced Textbooks in Control and Signal Processing, Springer London, London, 2011, pp. 59–167.
[17] L. Tay-Wo-Chong, T. Komarek, R. Kaess, S. Föller, W. Polifke, in: Proceedings of the ASME Turbo Expo, in: GT2010-22769, ASME, Glasgow, UK, 2010, pp. 623–635, doi:10.1115/GT2010-22769.
[18] L. Tay-Wo-Chong, S. Bomberg, A. Ulhaq, T. Komarek, W. Polifke, *J. Eng. Gas Turb. Power* 134 (2) (2012) 021502–1–8, doi:10.1115/1.4004183.